The Influence of the Multi-level Structure Under High Drawing on the Preparation of High Strength Lyocell Fiber

Shiqiang Cui (519476124@qq.com)
Donghua University - Songjiang Campus: Donghua University
Yang Zhang
Donghua University
Changjun Liu
Chtc Helon (Weifang) New Materials Co., Ltd.
Shanhao Lou
Chtc Helon (Weifang) New Materials Co., Ltd.
Yue Zhang
Donghua University
Yumei Zhang
Donghua University
Huaping Wang
Donghua University

Research Article

Keywords: Lyocell, draw ratio, multi-level structure, WAXD, SAXS

Posted Date: June 30th, 2021

DOI: https://doi.org/10.21203/rs.3.rs-571075/v1

Version of Record: A version of this preprint was published at Cellulose on January 16th, 2022. See the published version at https://doi.org/10.1007/s10570-021-04364-x.

The influence of the multi-level structure under high drawing on the preparation of high strength Lyocell fiber

Shiqiang Cui[a], Yang Zhang[a], Changjun Liu[b], Shanhao Lou[b], Yue Zhang[a,*], Yumei Zhang[a,*], Huaping Wang[a]

(a: College of Materials Science and Engineering, Donghua University, State Key Laboratory for Modification of Chemical Fibers and Polymer Materials, Shanghai 201620, China; b: Chtc Helon (Weifang) New materials Co., Ltd., Shandong Province 261000, China)

*correspondence to: Yumei Zhang, E-mail: zhangym@dhu.edu.cn Tel/Fax: 0086-21-67792957; Yue Zhang, E-mail: zhangyue@dhu.edu.cn

Abstract:

In order to research the multi-level structure of Lyocell fiber at different draw ratios and to reveal the limiting factors for preparing the high strength Lyocell fiber, the paper reports on the effect of draw ratio including low drawing (1-5), high drawing (6-11) and excessive drawing (12-20) on the multi-level structure and the mechanical properties of Lyocell fiber. The structure was determined by wide-angle X-ray diffraction, small-angle X-ray scattering and fibrillation test, and the result showed that, at low draw ratio stage, the breaking strength, yield strength and modulus of the fiber increased with the draw ratio owing to crystallinity as well as orientation increased while the micropore decreased, and there are almost no microfibrils on the fiber surface. At high draw ratio stage, the orientation of amorphous region increasing was the principal reason for the increase of fiber mechanical properties, and the micropores continued to decrease and a few short and thick microfibril was formed. At excessive draw ratio stage, the breaking strength remained constant mainly due to the basically unchanged crystallinity and orientation of the fibers, the yield strength and modulus decreased due to the slip of the highly crystallized and oriented elementary fibril. Meanwhile, the micropores still decreased and became much slenderer, the number of microfibrils increased and the microfibrils showed tenuous structure. It could be summarized that Lyocell fiber had the characteristics of multi-level structure, and the fundamental reason limiting the improvement of mechanical properties with draw ratio increase was the slip of elementary fibril.

Keywords: *Lyocell, draw ratio, multi-level structure, WAXD, SAXS*

Introduction

Lyocell fiber is known as one of the most representative green fiber in the 21st century due to its natural and renewable resource advantages, clean processing technology and degradable environmental friendliness. Lyocell fiber has the advantage of antistatic, hygroscopicity and comfortable wearing, and it is widely used in clothing, home textile and medical field (Ibrahim 2002; Medronho et al. 2012; Klemm et al. 2005; Chen et al. 2015). Furthermore, Lyocell fiber has much higher strength and modulus, especially the outstanding wet strength and wet modulus compared to ordinary viscose fiber since its invention due to its dry jet wet spinning forming process (Röder at al. 2013; Woodings 1995; Ganster et al. 2006). It can be inferred that Lyocell fiber could have made a further strength in mechanical properties, however, there is no Lyocell

fiber product with much more outstanding properties than high-strength viscose fiber up to now, which seems to be a subject worthy of further discussion.

There has been considerable research in Lyocell fiber to improve the mechanical properties during the past decade by using high degree of polymerization cellulose pulp, adding modifier to the solution and carrying thermal treatment on the fiber et al (Fink et al. 2014; Zhang et al. 2010a, b). However, cellulose pulp with high degree of polymerization makes dissolving and spinning difficult, and the addition of modifier may affect the recovery of NMMO (Zhang e al. 2010; Wendler et al. 2005; Wendler et al. 2008a, b). With regard to spinning process conditions, although there are many factors (such as air gap length, temperature and concentration of coagulation bath, spinning speed and so on) affecting properties of Lyocell fiber (Mortimer et al. 1996a, b; Duan et al. 1999; Shao et al. 2000), the most significant factor is the draw ratio under the premise of other process optimization. It is a common understanding of fiber preparation technology to obtain high crystallinity and high orientation fibers by increasing the draw ratio, so as to achieve the goal of high strength and high modulus. Is it the same for Lyocell fibers? Many researchers have studied the relationship between the draw ratio and the structure behaviors of Lyocell fiber (Loubinoux et al. 1987; Mortimer et al. 2008; Kong et al. 2005; Hauru et al. 2014, Jiang et al. 2012). Mortimer and his coworkers have made great effort to investigate the influence of physical process parameters on the structure formation of Lyocell fiber (Mortimer et al. 2008). It was found that the breaking strength and modulus increase to a plateau region with draw ratio increase and they attributed this change to the maximum crystallization and orientation, which was same to Kong and Lauri' results (Kong et al. 2005; Hauru et al. 2014). However, it obviously cannot explain the fact that the fiber diameter (or fineness) decreases with draw ratio increase. It has long been known, different types of regenerated cellulose fibers (such as viscose fiber, modal fiber and Lyocell fiber) are composed of elementary fibril which is consisted of cellulose II lamellar crystal and low ordered cellulose molecules in the form of string beads, and the microfibrils are comprised of elementary fibril and the micropores between the elementary fibril (Lenz et al. 1988; O'Sullivan 1997; Blackwell et al. 1975; Schurz et al. 1994; Statton 1956; Moss et al. 2010); it means that there are some other structure variations at different levels besides crystallization and orientation, which have a very remarkable impact on the mechanical properties in the process of spinning.

High performance regenerated cellulose fiber can be used in tire cord, carbon fiber precursor and other industrial fields, however, the mechanical properties are still the bottleneck for the application in industrial field of Lyocell fibers (Zhang et al. 2010; Peng et al. 2003). The investigated on the multi-level structure change of Lyocell fiber with draw ratio increasing is of great importance to understand the essential reason that limit the mechanical properties improvement, meanwhile, it can provide guidance for the improvement of Lyocell preparation process and fiber properties. The present study aimed at determining the multi-level structure of Lyocell fiber with draw ratio increasing, providing a basis for understanding the change of mechanical properties in terms of structural features. The structure evolution mechanism in terms of low drawing, high drawing and excessive drawing was proposed according to wide angle X-ray scattering (WAXD), small angle X-ray scattering (SAXS), birefringence, scanning electron microscope (SEM) combined with fibrillation test.

Experimental

Materials

Wood pulp (7.15 w t% water content, DP=550, α-cellulose content was 91%) was provide by COSMO Specialty Fibers, Inc, and N-methylmorpholine-N-oxide (NMMO) aqueous solution was bought from Amines & Plasticizers Limited with initial water content of 50 w t%. The propyl gallate (PG) was used as a stabilizer and was bought from Aladdin Industrial Corporation.

Preparation of cellulose solution

The NMMO aqueous solution was mixed with cellulose pulp and propyl gallate (PG), after swelling at 50 ˚C for one hour, the mixture was dissolved at 90 ˚C in a planetary stirred tank with a vacuum pressure was -99 kpa. The final solution was composed of 10 w t% cellulose, 78 w t% NMMO and 12 w t% water.

Preparation of regenerated cellulose fibers

A customized spinning equipment was used to prepared the Lyocell fibers and the schematic diagram of spinning process is shown in Fig.1. The spinning temperature was 90 ˚C, the specification of spinneret is 60 holes * 0.1mm, and the air gap length was 50 mm with a relative humidity of 65% and temperature of 25 ˚C. The concentration of NMMO in coagulation bath is 20 w t% and temperature of coagulation bath is 25 ˚C. Then, the solvent in filament was washed out in 60 ˚C hot water bath and 100 ˚C boiling water bath, and finally dried in 105 ˚C for 30 min to obtain fiber samples. 20 samples were prepared with different draw ratios by keeping the extrusion speed (6m/min) constant, adjusted the speeds of the first drawing roller.

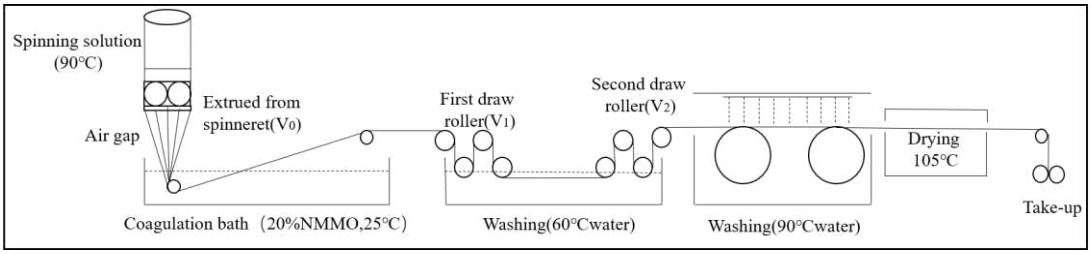

Fig. 1 Schematic diagram of Lyocell fiber spinning process

Measurements

The diameter of single filaments of all samples was measured by optical microscope (8XB-PC, China), and the breaking strength, yield modulus and initial modulus of Lyocell fibers were measured on a monofilament strength tester at least 30 measurements for each sample, and the drawing rate was 20 mm/min.

The fiber cross-section was observed on a scanning electron microscope, and the cross-sections of the fibers were observed after gold spraying treatment.

The WAXD measurements of the fibers were performed on the BL14B1 beam line of Shanghai Synchrotron Radiation Facility at a wavelength of 0.124 nm (Yang et al., 2015). The

distance between sample and detector of WAXD is 329.4mm. And the X-polar (Precision works NY, Inc., USA) was used to analysis the data include background correction, radial and azimuth integration. (Jiang et al 2012; Yuan et al; Chen et al., 2019).

The crystallinity is determined by the equation (1):

$$X_c = \frac{S_c}{S_a + S_c} \times 100\% \quad (1)$$

where X_c, S_c and S_a represent the crystallinity, the peak areas of crystalline phases and the peak areas of amorphous phases respectively.

The Scherrer equation was used to calculate the crystal size of Lyocell fibers (Jiang et al. 2012).

$$L_{hkl} = \frac{K\lambda}{\beta cos\theta} \quad (2)$$

where L_{hkl} represents the crystal size of (*hkl*) plane, λ is 0.124 nm in this experiment, 2θ is the diffraction angle (2θ), β is the integral width corresponding to the diffraction peak of crystal plane and *K* is 0.9 in this experiment.

The orientation of crystal region was determined from the equation (3) (Klug and Alexamder 1954):

$$f_c = (3\langle \cos^2 \varphi_{c,Z} \rangle - 1)/2 \quad (3)$$

where $< cos^2 \varphi_{c,Z} >$ is orientation parameter of crystal axis (*c*) relative to the fiber axis (*Z*).

The orientation parameter $< cos^2 \varphi_{c,Z} >$ was obtained according to the Wilchinsky Model (1959) and crystal symmetry of regenerated cellulose fibers (Kolpak and Blackwell 1976). For Lyocell fiber, the reflections in equatorial (*110*), (*020*) and (*-110*) were used to calculate the orientation parameter $< cos^2 \varphi_{c,Z} >$, and for each reflection (*hkl*), the orientation parameter $< cos^2 \varphi_{hkl} >$ can be determined by equation (4) and (5) (Klug and Alexamder 1954):

$$< cos^2 \varphi_{hkl} >= cos^2 \theta < sin^2 \varphi_{hkl} > \quad (4)$$

$$< sin^2 \varphi_{hkl} >= \frac{\int_0^{\pi/2} I(\varphi_{hkl}) \, sin^2 \varphi_{hkl} \, cos \varphi_{hkl} d\varphi_{hkl}}{\int_0^{\pi/2} I(\varphi_{hkl}) \, cos \varphi_{hkl} d\varphi_{hkl}} \quad (5)$$

where φ_{hkl} is the azimuthal angle and I (φ_{hkl}) is the diffraction intensity along the reflection plane (*hkl*).

The birefringence (Δn) was determined on polarizing microscope (type SSY-C).

The orientation factor (f_a) of amorphous region was calculated by Stein equation (6):

$$f_a = \frac{\Delta n - X_c \cdot \Delta n_c^0 \cdot f_c}{(1 - X_c) \cdot \Delta n_a^0} \quad (6)$$

where Δn represents the birefringence of Lyocell fibers, X_c represents the crystallinity, Δn_{co} is the birefringence index of the crystalline regions with a value of 0.0545, and Δn_{ao} is the birefringence index of amorphous regions as 0.0545 (Peng et al. 2003).

The SAXS measurements were determined at BL16B beamline of Shanghai Synchrotron Radiation Facility with X-ray wavelength of 0.124 nm and a distance between sample and detector of 1,920 mm (Zeng et al. 2017). The detailed structure parameters of the fibers were obtained by the X-polar referred to the previous methods (Murthy and Grubb 2010; Wu et al. 2000; Jiang et al. 2007; Colombe et al. 2011).

For Lyocell fiber, it is generally accepted that the striae on the equator in the SAXS is caused by the scattering of the micropores along the fiber axis (Crawshaw et al. 2000; Vickers et al. 2001;

Chen et al. 2007). Therefore, Guinier functions can be used to calculated the transverse dimension of micropore as shown in equation (7) (Guinier and Fournet 1955):

$$I(q) = I(0)\, exp(-q^2R^2/5) \quad (7)$$

where R is the radius of micropores, q ($q = 4p\ sin\ \theta/\lambda$) represents the scattering vector, θ is half of the scattering angle and λ is 0.124 nm in this experiment.

And the average micropores length (L) and orientation deviation angle (B_Φ) which relative to fiber axis were obtained according to the method of Ruland (Ruland 1969).

The real density of the fiber is calculated by the crystallinity of Lyocell fiber (the crystal region density of Lyocell fiber is 1.585, the amorphous region density is 1.483), and the real density of the fiber is calculated from equation (8):

$$\rho_0 = 1.585 * X_c + 1.483 * (1 - X_c) \quad (8)$$

where X_c is the crystallinity of the fiber.

The apparent density of the fiber is calculated equation (9):

$$\rho_l = (4 * D) / (10000 * \pi * d\ \hat{}\ 2) \quad (9)$$

where D is the linear density of the fiber, and d is the fiber diameter.

The fibrillation behavior was determined by observing the morphology of the treated Lyocell fibers with an optical microscope after radiated the fiber surface for 30 min by ultrasonic wave (Yuan et al, 2019). The average length of fibril is obtained by processing the image and quantitatively calculated by equation (10):

$$L_f = \frac{1}{n}\sum_{i=1}^{n} l_i \quad (10)$$

Where L_f is the average fibril length, l_i is the fibril length, n is the total number of fibrils.

Results and discussion

Mechanical properties of Lyocell fibers with different draw ratios

As we all known, the diameter of the fiber decreased as the draw ratio increasing during spinning, which help to improve the mechanical properties of the fiber. It can be seen from Fig. 2(a) that the diameters of the fibers decreased non-linearly, and the data can be fitted according to the model proposed by Mortimer (Mortimer 1996), and a theoretical prediction of fiber diameter (d) could be calculated according to the draw ratio (D_R) as follows:

$$d = d_0 * D_R^{-a} \quad (11)$$

Where d_0 is the diameter of the spinneret, and the value of a is 0.50. The model is consistent with the data of this paper, and gave the value of d_0 and a is 41 μm and 0.51, respectively, which is basically the same as the value measured by Mortimer. Additionally, it can be seen that the diameter decreases obviously at first and then slowly with draw ratio increase.

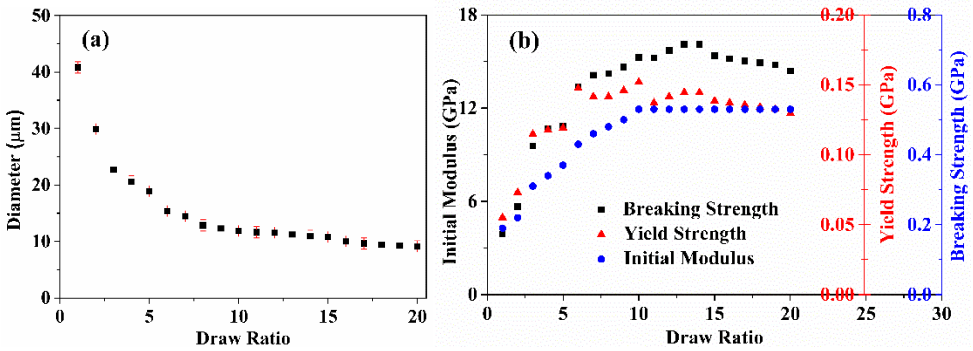

Fig. 2 Diameter (a) and mechanical properties (b) of Lyocell fibers with different draw ratios (1-20)

The mechanical data obtained from stress-strain curves (as shown in supporting information (Fig. S1)) of Lyocell fibers with different draw ratios are shown in Fig. 2(b). It can be seen that the breaking strength of Lyocell fiber gradually increases to a plateau area with draw ratio increasing to 12, while the modulus and yield strength increase first and then decrease slightly. Combined with the results of fiber diameter, the decrease of fiber diameter means the improvement of orientation and density, the mechanical properties of fibers should increase, but the actual result is obviously not like this. Normally, the mechanical properties of fibers are directly related to the structure, the difference between breaking strength, modulus and yield strength reflects the diversity of fiber structure, it can be said that there are some uncertain structures different from previous studies, which result in diameter of the fiber decrease with draw increase, while the breaking strength increases to a plateau and the modulus and yield strength increase first and then decrease. This paper will make a detailed study of its structural changes in the following.

Evolution of supramolecular structure of Lyocell fiber

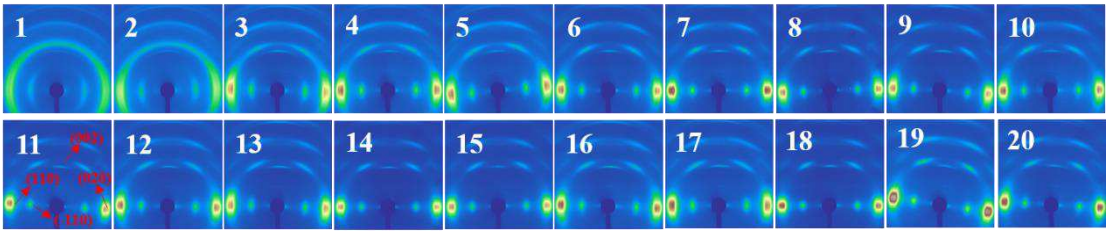

Fig. 3 WAXD patterns of Lyocell fibers with different draw ratios (1-20)

The crystal structural parameters of Lyocell fibers prepared at different draw ratio were calculated by analyzing the 2D WAXD patterns and the result was shown in Fig. 3. It can be seen that Lyocell fiber showed typical cellulose II crystalline structure and the diffraction pattern shown with the characteristic reflections of (*-110*), (*110*) and (*020*) crystal plane on the equator and the (*002*) crystal plane reflection in meridian. From Fig. 3, diffraction arcs became shorter as draw ratio increased which illustrates that the orientation of crystal region relative to fiber axis get better with draw ratio increasing, resulting in a higher orientation of Lyocell fibers. Subsequently, in order to further analyze the microstructure change, one-dimensional integral curves were obtained

by processing the two-dimensional WAXD patterns as shown in supporting information (Fig. S2), and the information of crystal and amorphous structural parameters as depicted in Fig. 4 were determined by fitted the one-dimensional intensity curves with six crystal peaks with the strongest diffraction and an amorphous peak according to the cellulose II crystalline structure which was shown at supporting information (Fig. S3). The crystallinity and crystal size of the fibers as shown in Fig. 4(a) and (b) indicated that the crystallinity of fibers increased with draw ratio increasing at low drawing stage, but remained constant at high and excessive drawing stage. The crystal size of (*-110*), (*110*) and (*020*) crystal plane on the equatorial line does not change significantly, while the crystal size of (*002*) crystal plane on the meridian direction increases significantly at low drawing stage, which was the principal reason for the raise of crystallinity

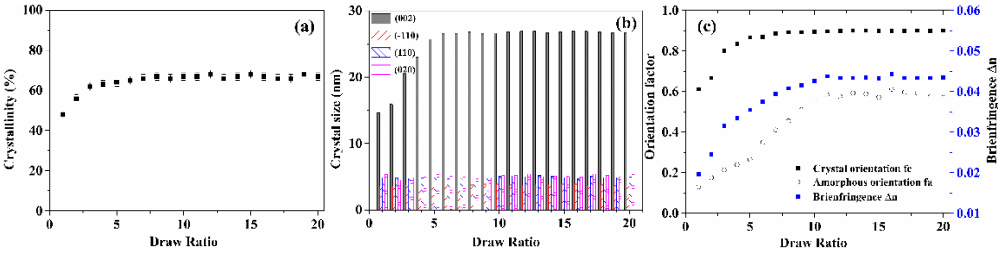

Fig.4 The supramolecular structure parameters of Lyocell fibers with different draw ratios (1-20): (a) crystallinity; (b) crystal size; (c) crystal orientation factor (f_c), amorphous orientation factor (f_a), birefringence index (Δn)

The orientation factor of crystal region (f_c), orientation factor of amorphous region (f_a) and birefringence index (Δn) were also obtained and shown in Fig. 4(c). The orientation of crystal regions and amorphous regions of Lyocell fibers as well as the birefringence index also increase with the draw ratio increasing. However, the increase of crystal orientation is mainly occurred at low drawing stage which is consistent with the change of crystallinity, while the increase of amorphous orientation and birefringence occurred at low and high drawing stage.

Evolution of fibril and micropore structure of Lyocell fiber

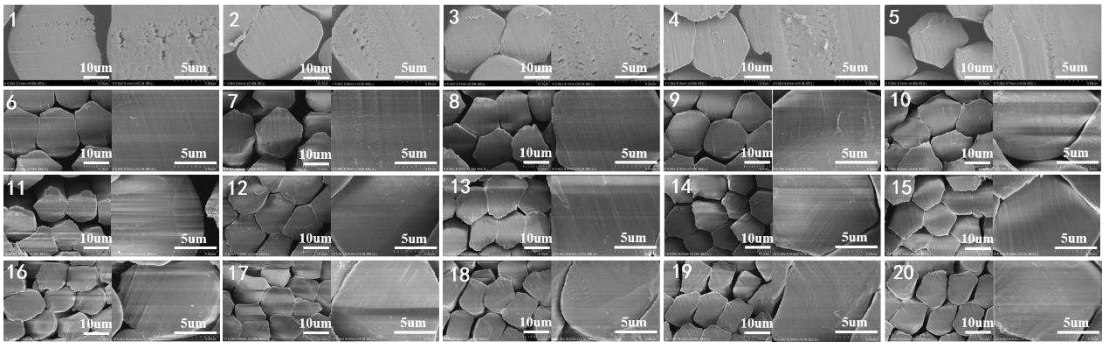

Fig. 5 SEM images of Lyocell fibers with different draw ratios (1-20)

In addition to the crystalline and orientation structure, the microstructure (such as hollows, micropores and microfibrils) in Lyocell fiber also has a very important impact on the mechanical properties (Blackwell and Kolpak 1975; Schurz and Lenz 1994; Statton 1956; Moss et al. 2010). The

morphological structure of the cross-sections of fibers was presented in Fig. 5. It can be observed that there were a few hollows with micron size in the fiber at low drawing stage, and the size of hollows gradually decreased at high and excessive drawing ratio, leading to the formation of the dense cross-section.

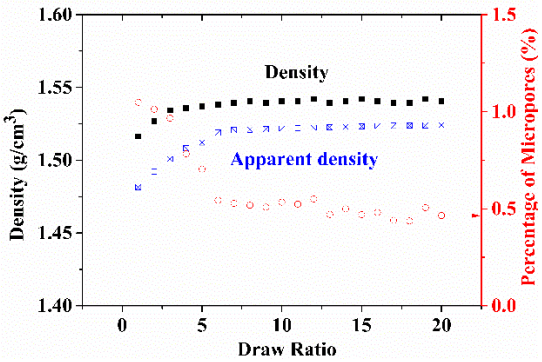

Fig. 6 The changes of the density and apparent density of Lyocell fibers with increasing draw ratios (1-20)

In addition to the micron-scale hollow, there are also some nano-scale micropore in Lyocell fibers, which is located between fibrils and fibrils according to the basic fiber model of cellulose fiber proposed by Schurz (Schurz and Lenz 1994). It is difficult to quantitatively analyze the nano-size variation by electron microscopy. Therefore, density method, SAXS technology and fibrillation test were used to study the evolution of micropore of Lyocell fiber during drawing.

The real density and apparent density of Lyocell fiber with draw ratio increase were calculated and shown in Fig. 6. It can be seen that compared to the real density, apparent density was smaller and increased much slower with the draw ratio increasing, indicating the existence of micropores in the fiber. The percentage of micropores volume was obtained by further calculating the apparent density and real density additionally shown in Fig. 6. it can be seen that the decrease trend of the percentage of micropores volume was similar to the increase trend of apparent density.

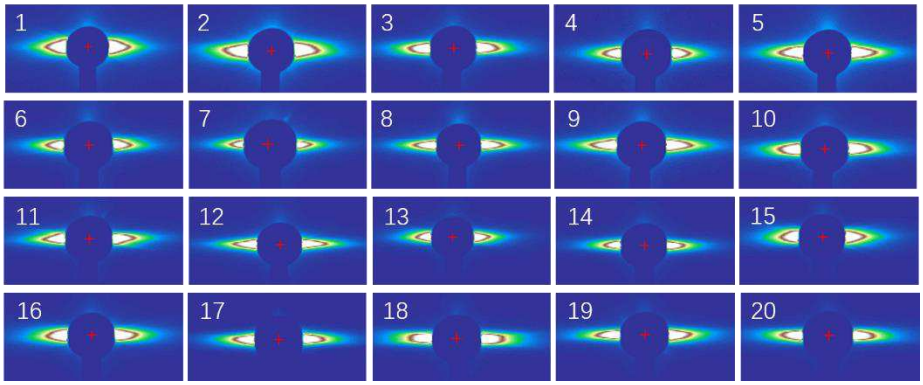

Fig. 7 SAXS patterns of the Lyocell fibers with different draw ratios (1-20)

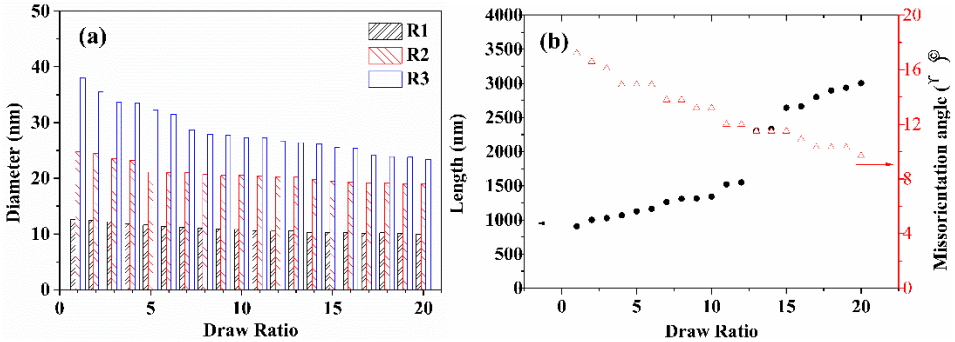

Fig. 8 Structural parameters from SAXS patterns of Lyocell fibers with different draw ratios (1-20): (a) micropores diameters; (b) micropores length and misorientation angle

The micropores of Lyocell fiber at different draw ratio were measured by SAXS as shown in Fig.7 in order to further investigated the microstructure evolution with the increase of draw ratio. The sharp and long striae on the equator in the SAXS is caused by the scattering of the micropores along the fiber axis, and additionally, the weaker and short striae on the meridian in SAXS patterns was due to the orientation and length of micropore in Lyocell fibers (Crawshaw et al. 2000). Based on the quantitative analysis of the two-dimensional SAXS scattering pattern, the micropore parameters of Lyocell fibers were calculated (The Guinier plot and Ruland plot of Lyocell fibers spun at different draw ratio were shown in supporting information (Fig. S4 and Fig. S5)), including micropore diameter, micropores length and micropore orientation deviation angle as shown in Fig. 8. It can be seen that the micropore in Lyocell fibers showed multi-level characteristics. The size of micropore decreased with draw ratio increasing, especially the larger micropore. The micropore length increased gradually while the orientation deviation angle of micropore decreased with draw ratio increasing especially at excessive drawing stage, indicating that the micropore get much longer and slenderer under drawing.

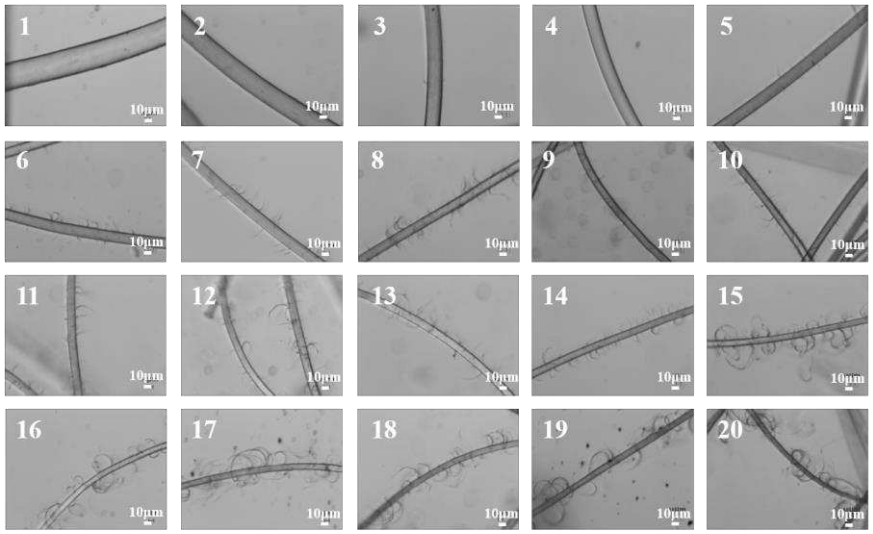

Fig. 9 The effect of draw ratios on fibrillation of Lyocell fibers

Table. 1 The effect of draw ratios on the average fibril length of Lyocell fiber

Low draw ratios	Draw ratios	1	2	3	4	5
	Average fibril length/μm	0	0	0	3.9	4.9

High draw ratios	Draw ratios	6	7	8	9	10	11
	Average fibril length/μm	7.8	9.1	10.1	10.6	11.3	11.5
Excessive draw ratios	Draw ratios	12	13	14	15	16	17	18	19	20
	Average fibril length/μm	12.4	12.8	12.9	20.0	22.5	22.8	24.6	31.3	34.3

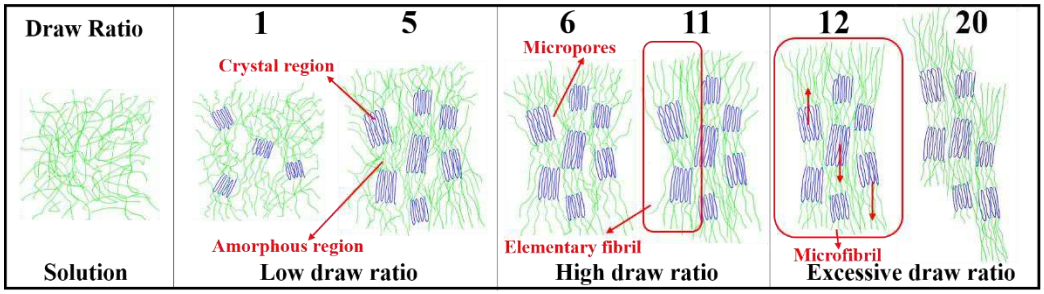

Fig.10 Schematic diagram to depict the evolution of Lyocell fiber microstructure with different draw ratios

The fibrillation of Lyocell fiber samples at different draw ratios was measured by radiated strong sonic wave on the fiber surface for 30min, the fibrillation and the average fibril length of Lyocell fiber was shown in Fig. 9 and Tab.1 respectively. In order to intuitively describe the differences in structure as well as the structural evolution of Lyocell fiber at different draw ratio, an appropriate structural model based on all the above tests was proposed, as shown in Fig. 10.

It can be seen that there was no obvious fibril on the fiber surface at low drawing stage due to the amorphous region with low degree of orientation increase the binding force of the elementary fibril. The increase of crystallinity and orientation lead to the increase of the breaking strength, modulus and yield strength of the fiber with the drawing ratio at low drawing stage.

At high drawing stage, the fibers form a highly crystalline and oriented structure, leading to the formation of microfibrils. Meanwhile, the length of the microfibrils increase is due to the raise of the amorphous orientation, which leads to the lengthening of the elementary fibrils as shown in Fig. 10, it can also be reflected by the variation of micropore structure. And the increase of the breaking strength, modulus and yield strength of the fiber with the drawing ratio at high drawing stage is mainly owing to the increase of amorphous orientation.

Moreover, it can be seen from Tab. 1 that the fibril length also increased with draw ratio especially when the draw ratio was above 15. Both of crystallinity and orientation of the fiber remained unchanged with draw ratio increase at excessive drawing stage while the length of micropores and microfibrils increase. This seems to be a contradictory problem, but the fact is the elementary fibrils slip due to weak interaction forces, which leads to the increase of the length of micropores and microfibrils as shown in Fig. 10. The structure of highly crystallized and oriented elementary fibrils keeps the breaking strength constant, but the slip of elementary fibrils leads to the decrease of modulus and yield strength.

Conclusions

Summarizing the changes of mechanical properties and structure of Lyocell fiber with different draw ratio, it can be concluded that, at low drawing stage, the increase of the breaking

strength, modulus and yield strength attributed to the raise of crystallinity and orientation, and the raise of crystallinity is mainly due to the increase of crystal region and crystal size perpendicular to the (002) crystal plane; at high drawing stage, the mainly reason for the breaking strength, modulus and yield strength increasing was the improvement of amorphous orientation; and at excessive drawing stage, the highly crystallized and oriented structure kept the breaking strength constant, while the decrease of modulus and yield strength was due to the elementary fibrils slipping caused by weak interaction. Therefore, the above structural defects limited the increase of fiber strength with the increase of draw ratio, in other words, there is a limitation to improve the mechanical properties by increasing the draw ratio in the current production process of Lyocell fiber, this suggests that further improvements must be made in the processing of Lyocell fibers.

Declaration

Conflict of interest

The author states that there are no competing economic interests.

Ethical approval

This paper does not cover studies of human participants or animals by all the authors.

Acknowledgements

Thanks for the support of the National Natural Science Foundation of China (51773032) and the help of Shanghai Synchrotron Radiation Facility (SSRF).

References

Blackwell J, Kolpak F J (1975). The cellulose microfibril as an imperfect array of elementary fibrils. Macromolecules 8(3):322-326.

Crawshaw J, Cameron R E (2000). A small angle X-ray scattering study of pore structure in Tencel ® cellulose fibers and the effects of physical treatments. Polymer 41(12):4691-4698.

Chen X, Burger C, Fang D, Hsiao B S, Chu B, Qi H, Zhang L (2007). Structure Development in Regenerated Cellulose Fibers Wet-Spun from Environmentally Friendly NaOH/Urea Aqueous Solutions Containing Cellulose I Crystals. J Biobased Mater Bio 1(2):266-273.

Colombe G, Gree S, Lhost O, Dupire M, Ivanov D A (2011). Correlation between mechanical properties and orientation of the crystalline and mesomorphic phases in isotactic polypropylene fibers. Polymer 52(24):5630-5643.

Chen J H, Guan Y, Wang K, Xu F, Sun R (2015) Regulating effect of hemicelluloses on the preparation and properties of composite Lyocell fibers. Cellulose 22(3):1505-1516.

Chen K, Yu J, Liu Y, Song M, Jiang Q, Ji H, Zou J, Zhang Y, Wang H (2019). Creep deformation and its correspondence to the microstructure of different polyester industrial yarns at room temperature. Polym Int 68(3):555-563.

Duan J, Shao H, Zhang T, Hu X (1999). Influences of NMMO content in coagulation bath on mechanical properties of Lyocell fibers. Journal of Donghua University (4):17-19.

Fink H P, Ganster J, Lehmann A (2014) Progress in cellulose shaping: 20 years industrial case studies at Fraunhofer IAP. Cellulose 21(1):31-51.

Guinier A, Fournet G, Walker C B, Vineyard G H (1956). Small-Angle Scattering of X-Rays. Phys Today, 1956, 9(8):38

Ganster J, Fink H P, Pinnow M (2006) High-tenacity man-made cellulose fibre reinforced thermoplastics injection moulding compounds with polypropylene and alternative matrices. Compos Part A: Appl Sci Manufac 37(10):1796-1804.

Gindl W, Martinschitz K J, Boesecke P, Keckes J (2006). Orientation of cellulose crystallites in regenerated cellulose fibers under tensile and bending loads. Cellulose 13(6):621-627.

Hauru L K J, Hummel M, Michud A, Sixta H (2014) Dry jet-wet spinning of strong cellulose filaments from ionic liquid solution. Cellulose 21(6):4471-4481.

Ibrahim M (2002) Preparation of cellulose and cellulose derivative azo compounds. Cellulose 9(3-4): 337-349.

Jiang Z, Tang Y, Men Y, Enderle H F, Rieger J (2007). Structural Evolution of Tensile-Deformed High-Density Polyethylene during Annealing: Scanning Synchrotron Small-Angle X-ray Scattering Study. Macromolecules 40(20):7263-7269.

Jiang G, Yuan Y, Wang B,Yin X, Mukuze K S, Huang W, Zhang Y, Wang H (2012) Analysis of regenerated cellulose fibers with ionic liquids as a solvent as spinning speed is increased. Cellulose 19(4):1075-1083.

Klug H, Alexamder L. X-ray diffraction procedures. Wiley, New York

Kolpak FJ, Blackwell J (1976) Determination of the structure of cellulose II. Macromolecules 9:273-278

Klemm D, Heublein B, Fink H P, Bohn A (2005) Cellulose: fascinating biopolymer and sustainable raw material. Angew Chem Int Ed 44:3358-3393.

Kong K, Eichhorn S J (2005) Crystalline and amorphous deformation of process-controlled cellulose-II fibres. Polymer 46(17):6380-6390.

Medronho B, Romano A, Miguel M G, Stigsson L Lindman B (2012) Rationalizing cellulose (in)solubility: reviewing basic physicochemical aspects and role of hydrophobic interactions. Cellulose 19(3):581-587.

Loubinoux D, Chaunis S (1987) An Experimental Approach to Spinning New Cellulose Fibers with N-Methylmorpholine-Oxide as a Solvent. Text Res J 57(2):61-65.

Lenz J, Schurz J, Wrentschur E (1988). The fibrillar structure of cellulosic man-made fibers spun from different solvent systems. J Appl Polym Sci 35(8):1987- 2000.

Mortimer S A, Peguy A A (1996). The influence of air-gap conditions on the structure formation of lyocell fibers. Journal of Applied Polym Sci 60(10):1747-1756.

Mortimer S A, A.A. Péguy (1996). The formation of structure in the spinning and coagulation of lyocell fibers. Cell Chem Technol 30(1):71-82.

Mortimer S A, Péguy A.A., Ball R C (2008) Influence of the physical process parameters on the structure formation of lyocell fibres. Cell Chem Technol 30(3):251-266.

Moss C E, Butler M F, M. Müller, Cameron R E (2010). Microfocus small-angle X-ray scattering investigation of the skin–core microstructure of lyocell cellulose fibers. J Appl Polym Sci

83(13):2799-2816.

Murthy N S, Grubb D T (2010). Tilted lamellae in an affinely deformed 3D macrolattice and elliptical features in small‐angle scattering. J Polym Sci Polym Phys 44(8):1277-1286.

O'Sullivan A C (1997). Cellulose: the structure slowly unravels. Cellulose 4(3):173-207.

Peng S, Shao H, Hu X (2003). Lyocell fibers as the precursor of carbon fibers. Journal of Applied Polym Sci 90(7):1941-1947.

Ruland W (2010). Small‐angle scattering studies on carbonized cellulose fibers. J Polymer Sci Polym Symp, 28(1):143-151.

Röder T, Moosbauer J, Wöss K, Schlader S, Kraft G (2013) Man-made cellulose fibres-a comparison based on morphology and mechanical properties. Lenzing Ber 91:7-12.

Statton W O (1956). Crystallite regularity and void content in cellulose fibers as shown by small-angle x-ray scattering. J Polym Sci 22(102):385-397.

Schurz J, Lenz J (1994). Investigations on the structure of regenerated cellulose fibers. Macromol Symp 83(1):273-289.

Shao H, Wang J (2000). Effects of coagulation bath conditions on crystal structure of lyocell fibers. Synthetic Fiber in China.

Vickers M E, Briggs N P, Ibbett R N, Payne J J, Smith S B (2001). Small angle X-ray scattering studies on lyocell cellulosic fibers: the effects of drying, re-wetting and changing coagulation temperature. Polymer 42(19):8241-8248.

Wilchinsky Z W (1959). Advances in X-Ray Analysis. J Appl Phys 30:782-789.

Woodings C R (1995) The development of advanced cellulosic fibres. Int J Bio Macromol 17(6):305-309.

Wu J, Schultz J M, Yeh F, Yeh F, Hsiao B S, Chu B (2000). In-Situ Simultaneous Synchrotron Small- and Wide-Angle X-ray Scattering Measurement of Poly(vinylidene fluoride) Fibers under Deformation. Macromolecules 33(5):1765-1777.

Wendler F, Kolbe A, Meister F, Heinze T (2005) Thermostability of lyocell dopes modified with surface- active additives. Macromolr Mater Eng 290: 826- 832.

Wendler F, Kolbe A, Kraft J, Einax J, Heinze T (2008) Thermal stability of lyocell solutions: experimental results and modeling using cluster analysis and partial least squares regression. Macromol Theor Simul 17: 32- 38.

Wendler F, Konkin A, Heinze T (2008). Studies on the stabilization of modified lyocell solutions. Macromol Symp 262: 72- 84.

Yang T, Wen W, Yin G, Li X, Gao M, Gu y, Li L, Liu Y, Lin H, Zhang X (2015). Introduction of the X-ray diffraction beamline of SSRF. Nucl Sci and Tech 26(2):020101.

Yuan W, Wu K, Liu N, Zhang Y, Wang H (2018). Cellulose acetate fibers with improved mechanical strength prepared with aqueous NMMO as solvent. Cellulose 25:6395-6404

Zhang H, Shao H, Hu X (2010) Effect of heat treatment on the structure and properties of Lyocell fibers. J Appl Polym Sci 101(3):1738-1743.

Zhang H, Wei M, Shao H, Hu X (2010) Effect of cellulose pulp on the properties of lyocell fiber used as tire cord. Journal of Donghua University, 36(5):486-480.

Zeng J, Bian F, Wang J, Li X, Wang Y, Tian F, Zhou P (2017). Performance on absolute scattering

intensity calibration and protein molecular weight determination at BL16B1, a dedicated SAXS beamline at SSRF. J Synchrotron Radiat 24(2):509-520

Supplementary Files

This is a list of supplementary files associated with this preprint. Click to download.

- SupportingInformation.docx